Physics and Imaging in Radiation Oncology 31 (2024) 100605

Contents lists available at ScienceDirect

Physics and Imaging in Radiation Oncology

journal homepage: www.sciencedirect.com/journal/physics-and-imaging-in-radiation-oncology

Original Research Article

Comparison of stereotactic radiotherapy and protons for uveal melanoma patients

Emmanuelle Fleury [a,b,*], Jean-Philippe Pignol [c], Emine Kiliç [d,e], Maaike Milder [a], Caroline van Rij [a], Nicole Naus [d], Serdar Yavuzyigitoglu [d], Wilhelm den Toom [a], Andras Zolnay [a], Kees Spruijt [b], Marco van Vulpen [b], Petra Trnková [a,f], Mischa Hoogeman [a,b]

[a] Erasmus Medical Center Cancer Institute, University Medical Center, Department of Radiotherapy, Rotterdam, The Netherlands
[b] HollandPTC, Delft, The Netherlands
[c] College of Medicine, Al Faisal University, Riyadh, Saudi Arabia
[d] Erasmus Medical Center, Department of Ophthalmology, Rotterdam, The Netherlands
[e] Erasmus Medical Center, Department of Clinical Genetics, Rotterdam, The Netherlands
[f] Medical University of Vienna, Department of Radiation Oncology, Vienna, Austria

ARTICLE INFO

Keywords:
Stereotactic radiotherapy
Proton therapy
Uveal melanoma
Imaging-based planning

ABSTRACT

Background and purpose: Uveal melanoma (UM) is the most common primary ocular malignancy. We compared fractionated stereotactic radiotherapy (SRT) with proton therapy, including toxicity risks for UM patients.
Materials and methods: For a total of 66 UM patients from a single center, SRT dose distributions were compared to protons using the same planning CT. Fourteen dose-volume parameters were compared in 2-Gy equivalent dose per fraction (EQD2). Four toxicity profiles were evaluated: maculopathy, optic-neuropathy, visual acuity impairment (Profile I); neovascular glaucoma (Profile II); radiation-induced retinopathy (Profile III); and dry-eye syndrome (Profile IV). For Profile III, retina Mercator maps were generated to visualize the geographical location of dose differences.
Results: In 9/66 cases, (14 %) proton plans were superior for all dose-volume parameters. Higher T stages benefited more from protons in Profile I, especially tumors located within 3 mm or less from the optic nerve. In Profile II, only 9/66 cases resulted in a better proton plan. In Profile III, better retina volume sparing was always achievable with protons, with a larger gain for T3 tumors. In Profile IV, protons always reduced the risk of toxicity with a median RBE-weighted EQD2 reduction of 15.3 Gy.
Conclusions: This study reports the first side-by-side imaging-based planning comparison between protons and SRT for UM patients. Globally, while protons appear almost always better regarding the risk of optic-neuropathy, retinopathy and dry-eye syndrome, for other toxicity like neovascular glaucoma, a plan comparison is warranted. Choice would depend on the prioritization of risks.

1. Introduction

Uveal melanoma (UM) patients are commonly treated with either surgery, photon-based stereotactic radiotherapy (SRT) [1–11], plaque brachytherapy, or proton therapy. UM is a standard indication for proton therapy [12] with a 5-year local control rate of more than 90 % worldwide [13–17]. Brachytherapy [18–21] and SRT [2,5,7,10,22,23] result in 5-year local control of 75–95 %. The selection among those techniques is based on the availability of a specific treatment modality, the ocular team experience, patient's preferences, and/or reimbursements. Differences in outcomes are still debated [24,25] and up to 70 % of adverse events have been reported after any radiotherapy [26]. As more centers treat UM with photon-based SRT and the number of proton centers worldwide increases, the patient selection based on the potential trade-off in toxicities needs to be addressed. The choice of the optimal technique should account for both the risk of post-treatment complications [26] and quality-of-life [27]. However, direct photon-proton plan comparison studies are not possible due to differences in treatment planning. Proton planning is historically based on a generic geometrical model [28], while SRT utilizes a CT-based planning

* Corresponding author at: Dr. Molewaterplein 40, 3015 GD Rotterdam, The Netherlands.
E-mail address: e.fleury@erasmusmc.nl (E. Fleury).

https://doi.org/10.1016/j.phro.2024.100605
Received 22 January 2024; Received in revised form 21 June 2024; Accepted 25 June 2024
Available online 26 June 2024

approach.

This study aimed to evaluate the differences in dose-volume metrics between SRT and proton therapy for UM patients using a CT-based *in-silico* planning comparative study. Four toxicity-specific profiles, representing the most clinically relevant complications, were compared to evaluate the potential benefit of each treatment option.

2. Materials and methods

2.1. Study population

Clinical baseline characteristics and treatment details of 66 UM patients (40 left, 26 right eyes) treated between 2016 and 2021 at Erasmus Medical Center (Rotterdam, The Netherlands) with SRT using a robotic CyberKnife M6 (Accuray, Sunnyvale, CA, USA) are summarized in Table 1. The local Ethics Committee approved the study (MEC-2021-0454). Tumors were classified using the American Joint Committee on Cancer (AJCC) staging [29]: 15 T1, 25 T2 and 26 T3. The median tumor apical height was 5.5 mm (range: 1.8–12.8 mm) and median volume was 0.4 cm^3 (range: 0.1–1.7 cm^3). Tumor apical height and largest basal diameter were retrieved from B-scan ultrasonography before irradiation. A planning CT was acquired at straight gazing angle with a voxel resolution of (0.59x0.59x1) mm^3. Anterior segment, retina (1-mm inset from the external eye globe until ora serrata), eye globe, vitreous body, optic nerve, optic disc, and lacrimal gland were manually contoured. As the macula was not discernible on CT or MRI, it was geometrically reconstructed based on fundus photography. For patients suffering from vitreous hemorrhage, the macula was defined at the intersection between the optical axis and retina. Registered MRI was used for delineation of the Gross Tumor Volume (GTV) when available.

Table 1
Baseline patient characteristics and treatment details.

Study population			
Age at diagnosis (mean ± SD, in years)			67.3 ± 13.2
Gender (n(%))	Female		27 (41 %)
	Male		39 (59 %)
Eye (n(%))		OS	40 (60.6 %)
		OD	26 (39.4 %)
Tumor characteristics			
LBD (median [range], in mm), (on US)			11.42 [4.34; 16.84]
Apical height (median [range], in mm), (on US)			5.51 [1.84; 12.80]
Tumor size classification AJCC T (n(%))			
	T1		15 (22.7 %)
	T2		25 (37.9 %)
	T3		26 (39.4 %)
Size of GTV (median [range], in cm^3)[a]			0.36 [0.07; 1.65]
Minimum distance tumor edge to organs-at-risk (median [range], in mm)			
	Fovea (on US)		2.00 [0.00; 12.00]
	Optic nerve [a]		2.59 [0.00; 18.84]
	Optic disc [a]		1.79 [0.00; 17.74]
	Anterior segment [a]		5.67 [0.00; 13.98]
	Lacrimal gland [a]		4.06 [0.00; 20.03]
Treatment details			
Fractionated stereotactic radiotherapy (SRT)			
	Prescription dose (RBE-weighted, in Gy)		50
	No. of fractions		5
	No. of beams (mean ± SD)		62.86 ± 21.66
	Iris collimator		59/66 cases (sizes: 7.5, 10, 12.5, 15 and/or 20 mm)
	Multileaf collimator		7/66 cases
	Beam-on time [b] (mean ± SD, in min)		21.65 ± 3.62
	Gazing angle		Straight [c]
	Monitor Units (delivered plans, mean ± SD)		2951.83 ± 964.81
Proton therapy			
	Prescription dose (RBE-weighted, in Gy)		60
	No. of fractions		4
	No. of beams		1
	Beam-on time		~ 1 min
	Ocular motility limits (gazing angle)		[−30; 30] degrees
	Monitor Units		NA [d]

[a] CT-based measurements; [b] Including a 5 min patient setup; [c] Fixation light usually placed at the center of the pupil of the treated or healthy eye; [d] Cannot be determined from the clinical TPS, within current clinical practice in ocular proton therapy using a dedicated eyeline.
Abbreviations: SD = Standard Deviation; LBD = largest basal diameter; US = ultrasound; AJCC = American Joint Committee on Cancer staging consensus [30]. SRT = fractionated stereotactic radiotherapy; GTV = gross tumor volume; TPS = treatment planning system.

2.2. Stereotactic radiotherapy

The relative biological effectiveness (RBE)-weighted dose of 50 Gy [23] (5x10 Gy) was prescribed to the 80 % isodose encompassing the Planning Target Volume (PTV) according to the International Commission of Radiation Units and Measurements (ICRU) Report 91 guidelines [30]. PTV included GTV with a 2-mm isotropic margin derived upon a multidisciplinary local consensus based on the assessment of uncertainties. At least 98 % of PTV received 95 % of the prescribed dose, resulting in a PTV near-maximum dose of 62.5 Gy (RBE-weighted = 1.0). Dose was calculated in Accuray Multiplan™ (Accuray, Sunnyvale, CA, USA) and delivered with a robotic CyberKnife M6 using either an iris collimator (range: 7.5 to 20 mm) or a multi-leaf collimator. To compensate for intrafraction patient motion, the 6D skull tracking method was used with tight rotational and translational boundaries. To mitigate eye setup errors, gating using a modified version of the Rotterdam Gill-Thomas-Cosman frame [31] with the camera and LED placed on an arch attached to a double-shell mask was employed.

2.3. Simulation of proton therapy

The prescription dose for proton therapy was 60 Gy (4x15 Gy, RBE-weighted = 1.1) within the treatment field where 100 % of dose was defined from the average dose within this treatment field according to ICRU Report 78 [32], resulting in at least 95 % of GTV receiving 90 % of the prescribed dose. Following an international consensus in ocular proton therapy [13,14,33–37], a 2.5-mm expansion was applied proximally and distally along the beam central axis to define the Spread-Out Bragg Peak. Laterally, a collimator encompassing the GTV with 2.5-mm margin was used, enabling at least 50 % of dose within the aperture. An optimal gazing angle to minimize organs-at-risk exposure and maximize treatment conformity was selected. Since the CTs were not performed at the optimal gazing angle, a composite transformation overlaid the simulated proton dose onto the planning CTs. The detailed description of the in-house dose algorithm used in this study is reported elsewhere [38,39].

2.4. Plan comparison and statistical analysis

Analysis accounted for the AJCC T staging, toxicity-specific profiles, and distance to the optic nerve. Four post-treatment complications profiles and relevant dose-volume parameters were evaluated [16,40–42]:

- **Profile I)** Maculopathy, optic-neuropathy, and visual acuity impairment: $D_{2\%}$, D_{mean} and V_{30Gy} to the optic nerve, D_{mean} to the optic disc, and $D_{2\%}$ to the macula;
- **Profile II)** Neovascular glaucoma: $D_{2\%}$ and D_{mean} received by the anterior segment, and the $D_{2\%}$ to the optic nerve;
- **Profile III)** Radiation-induced retinopathy: $D_{20\%}$ dose and V_{5Gy}, V_{10Gy}, V_{20Gy}, V_{30Gy} volumes to the retina;

- **Profile IV)** Dry-eye syndrome: $D_{2\%}$ and D_{mean} to the lacrimal gland.

For Profile I, all patients were categorized based on the distance from the tumor edge to the optic nerve, using a 3-mm threshold corresponding to a standard value globally reported for lateral and distal penumbrae with ocular beamlines [43–45]. The complications severity ranking followed our institutional multidisciplinary consensus.

A radiobiological equivalent dose of 2-Gy fractions (EQD2) with a 10 Gy α/β ratio for UM was calculated: RBE-weighted EQD2 prescribed dose was 83 Gy for SRT and 125 Gy for protons. $D_{2\%}$, $D_{20\%}$ and D_{mean} were also converted to RBE-weighted EQD2 using α/β of 2 Gy for the optic nerve, optic disc, macula, retina, anterior segment, and 3 Gy for the lacrimal gland. These values were based on the values reported by Joiner *et al* [46] and determined through a multidisciplinary consensus at HollandPTC (Delft, The Netherlands) to be used clinically. Dose-volume calculations for SRT and protons were performed with the in-house software Mattherhorn to avoid bias. Differences in RBE-weighted EQD2 dose between SRT and protons were calculated for every patient of the present cohort; and the EQD2-median of those differences used for comparison. This study followed the RATING guidelines [47].

3D retina dose surface maps, incorporating real retinal CT-based imaging, were created to enable a quantitative anatomical comparison in terms of exposed area. Additionally, 2D planar maps for surface dose were generated following the method described by Hoogeman *et al* [48]. Mercator dose projections of the retina surface were made from the centroid of each plane in the vitreous body with the outer retina perimeter of each plane segmented using a fixed number of 360 points evenly spaced. The 2D maps were expressed in RBE-weighted dose and RBE-weighted EQD2 dose.

Two-sided Wilcoxon signed-rank tests were used to evaluate the statistical significance of observed differences. Because of multiple tests, the significance was defined as $p < 0.01$. Analyses were performed using Python v3.7 and the SciPy package.

3. Results

All plans for both modalities achieved adequate target coverage. For all patients, 98 % of PTV received at least 95 % of the SRT dose. With protons, GTV received at least 90 % of the prescribed dose. Median RBE-weighted GTV D_{mean} was 59.6 Gy (range: 57.0–61.3 Gy) for SRT and 59.0 Gy (range: 57.6–59.6 Gy) for protons (Table 1). Average RATING score calculated by two authors (P.T, E.F.) was 82 %.

Patient examples and the associated comparisons are presented in Fig. 1 and Fig. 2. Comparative evaluation of dose-volume parameters is reported in Table 2 and Figure S1 in Supplementary Material, and graphically shown in Fig. 3 using AJCC-specific population-averaged spider maps. Superior proton plans for all 14 dose-volume metrics were in 9/66 patients. In 57/66 patients, some dose-volume parameters were favorable to SRT and some to protons, depending on the evaluated dose-volume metric.

For Profile I, EQD2-median differences between both modalities were all statistically significant in favor of protons, except for the maculopathy (Table 2). In 36/66 patients, the tumor border was located within 3-mm distance from the optic nerve, with a median minimum distance of 1.2 mm. All dose differences were favorable to protons: EQD2-median reduction of 44.1, 6.1 and 30.5 Gy for optic disc D_{mean}, optic nerve D_{mean} and optic nerve $D_{2\%}$, respectively (Tables S2). The higher AJCC T staging, the larger the dosimetric gain, with a maximum EQD2-median D_{mean} to the optic disc of 41.2 Gy for T1 and 72.0 Gy for T3 tumors. For the other 30/66 patients, the median minimum distance to the tumor edge was 5.6 mm and the proton EQD2-median optic nerve $D_{2\%}$ reduction was 17.8 Gy (Tables S2). Regarding AJCC T staging, EQD2-median macula $D_{2\%}$ was reduced with protons by 7.0 Gy for T1 tumors, 11.1 Gy for T2 tumors, and 19.9 Gy for T3 tumors. Independent of tumor location, there was no median optic nerve V_{30Gy} difference observed between protons and SRT.

For Profile II, an EQD2-median anterior segment $D_{2\%}$ and D_{mean} reduction of 114.5 Gy ($p < 0.01$) and 9.0 Gy ($p < 0.013$), respectively, was achievable with SRT over all patients (Table 2). Protons decreased

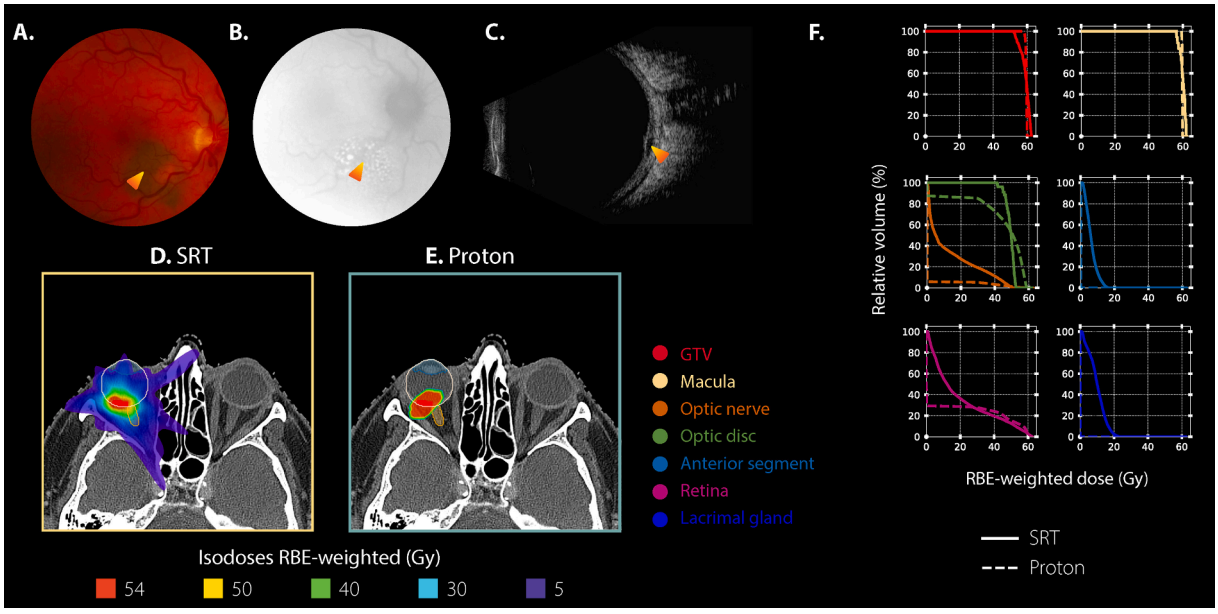

Fig. 1. Case example of an 80-year-old female patient diagnosed with an AJCC T1-staged choroidal melanoma in her right eye. **A, B, C)** Ophthalmic images at diagnosis. The orange-shaded arrow indicates the lesion. **A:** Fundus photography. **B:** Fluorescent angiography. **C:** B-scan ultrasound. Dimensions on ultrasound were of 7.2 mm for largest basal diameter and of 2.1 mm for tumor apical height. **D, E)** Axial dose distributions shown on the planning CT in respect to the gazing angle hold by the patient during the scan. For proton simulation, a gazing angle [$\Psi = 30$ degrees; ϕ=30 degrees] was considered. Ψ represented any elevation/depression of the eye, whereas ϕ represented any ab-/adduction. **F)** DVH results for both modalities, stereotactic radiotherapy (SRT) in solid line and proton in dashed line. Results are presented for a total treatment dose, in RBE-weighted dose (in Gy), or percentage of irradiated volume (%-point). (For interpretation of the references to colour in this figure legend, the reader is referred to the web version of this article.)

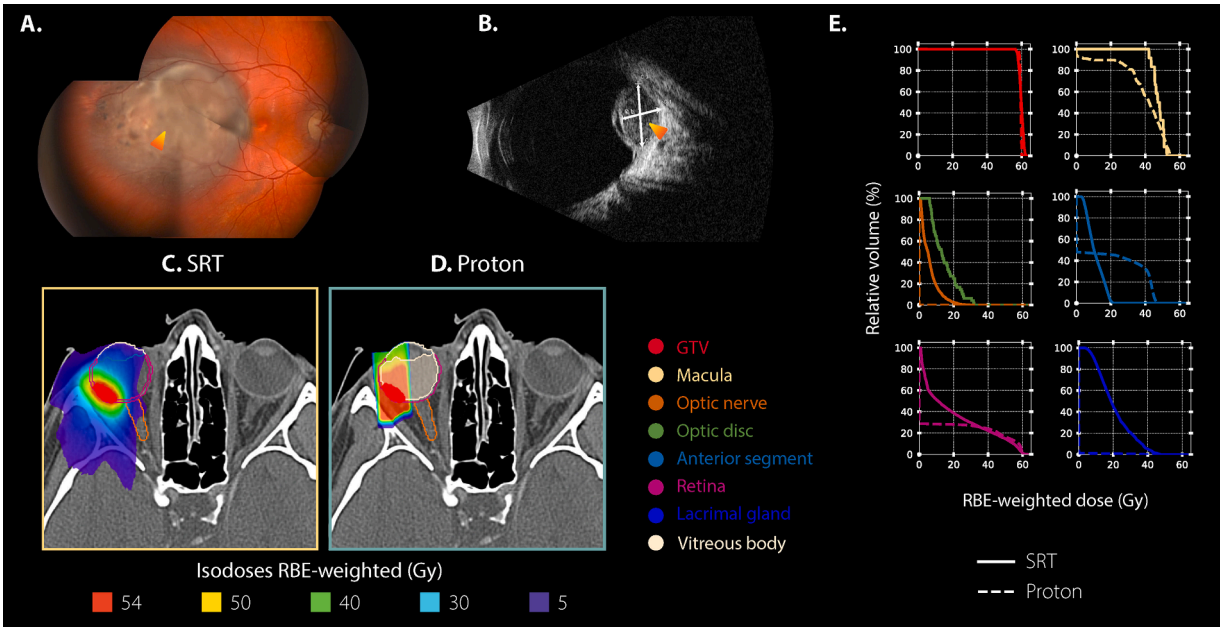

Fig. 2. Case example of a 21-year-old female patient diagnosed with an AJCC T2-staged choroidal melanoma in her right eye. **A, B)** Ophthalmic images at diagnosis. The orange-shaded arrow indicates the lesion. **A:** Fundus photography. **B:** B-scan ultrasound. Dimensions on ultrasound were of 8.4 mm for largest basal diameter and of 5.3 mm for tumor apical height. **C, D)** Axial dose distributions shown on the planning CT in respect to the gazing angle hold by the patient during the scan. For proton simulation, a straight gazing angle [$\Psi = 0$ degrees; ϕ=0 degrees] was considered. Ψ represented any elevation/depression of the eye, whereas ϕ represented any ab-/adduction. **E)** DVH results for both modalities, stereotactic radiotherapy (SRT) in solid line and proton in dashed line. Results are presented for a total treatment dose, in RBE-weighted dose (in Gy), or percentage of irradiated volume (%-point). (For interpretation of the references to colour in this figure legend, the reader is referred to the web version of this article.)

the optic nerve $D_{2\%}$ by an EQD2-median of 18.0 Gy ($p < 0.01$) compared to SRT. At patient's level, 9/66 cases had better dose distribution with protons based on the optic nerve $D_{2\%}$, and the anterior segment $D_{2\%}$ and D_{mean}. A minimum tumor edge to optic nerve distance was > 3-mm in 8/9 cases with variability in tumor patterns.

For Profile III, large variations were observed across all patients, with retina $D_{20\%}$ sometimes favorable to SRT and sometimes to protons, but not statistically significant due to interpatient variability (Figure S2). Importantly, retina $D_{20\%}$ was linked to AJCC staging, suggesting an advantage with protons for small T1 tumors with an EQD2-median dose reduction of 14.2 Gy, but a median increase of 42.0 Gy for T3 tumors. There was a tendency of a more pronounced retina volume sparing for T3 tumors compared to T1-T2 tumors with protons. Since dose-volume-histograms lose geographical information, Mercator projections enabled visualizing the differences between modalities at a patient's basis. Fig. 4 shows local EQD2 differences between blue zones, in favor of SRT, and red zones, in favor of protons. For the two patients represented, the blue zone appears similar to the red zone, despite lower retina V_{5Gy} to V_{20Gy} with protons (Figs. 1, 2, 3).

For Profile IV, an EQD2-median lacrimal gland D_{mean} reduction of 15.3 Gy was observed with protons ($p < 0.01$) for all patients. AJCC staging had no impact. As expected, larger dose differences were observed for the 42 temporal tumors (Table S3 & Figure S4). For this subgroup, the proton D_{mean} EQD2-median reduction was 22.8 Gy. At individual level, 36/42 patients presented a dosimetric gain with protons. For the 24 nasal tumors, the proton D_{mean} EQD2-median reduction was 5.5 Gy. At individual level, all 24 patients presented a dosimetric gain with protons. Interestingly, lacrimal gland $D_{2\%}$ showed large interpatient variability with no significant differences at Wilcoxon test (Figure S3).

4. Discussion

This study evaluated the differences in dose-volume metrics between protons and CyberKnife-based SRT for the same cohort of UM patients. Such comparison is *a priori* difficult because of differences in imaging for planning (ultrasound for protons vs. CT for SRT) [28,49–51] and in underlying technologies. Moreover, treatment fractionation, dose prescription and RBE also differ, making direct comparison challenging. Therefore, an isoeffective CT-based planning process with both specific GTVs receiving an RBE-weighted D_{mean} of 60 Gy was implemented to ensure an objective comparison. In general, GTV coverage with both protons and SRT was 100 %, except for a few proton cases where coverage was marginally less than 100 %, attributed to uncertainties in calculating the minimum dose due to the finite voxel size. The RBE-weighted EQD2-median dose were much higher for protons. Further discussions on prescription protocols for imaging-based planning in ocular proton therapy are needed to address these differences.

A correlation between radiation-related complications, the size of the tumor, and its proximity to sensitive ocular structures like the optic nerve or the macula/fovea was previously reported [52]. The vision (Profile I) might be irreversibly compromised after radiation-induced maculopathy and optic-neuropathy [53]. In our data, proton plans were dosimetrically superior to SRT in parameters related to vision impairment [50] with a benefit more pronounced for T3 tumors than T1-2 and less pronounced for tumors located adjacent to the optic nerve/disc, similar to other studies [17,54]. In a retrospective, non-randomized study comparing radiosurgery with protons, Sikuade *et al* reported on better visual acuity preservation with proton compared to radiosurgery [55]. Interestingly, while it is well-established that doses above 50 Gy lead to optic neuropathy [53], the optic nerve continues to be delineated as a straight tube of a few millimeters in diameter for proton planning. This segment of the optic nerve is particularly vulnerable to radiation damage, owing to its lack of myelin sheathing [56]. In our study, imaging-based planning was used for both treatment modalities, more precise evaluation of the dose distribution along the entire length of the optic nerve was possible. Such an accuracy in dose assessment during treatment planning could potentially contribute to the preservation of some visual function [26,57]. Additionally, biomechanical modelling could improve accuracy of gazing-angle specific optical nerve shape and

Table 2
Dosimetric findings (RBE-weighted dose or RBE-weighted EQD2 dose, or anatomical irradiated volume) across the cohort of patients. All values are expressed for a total treatment dose.

			Median RBE-weighted dose [range]				**RBE-weighted EQD2-median dose [range]**				**RBE-weighted EQD2-median difference [IQR]**		**RBE-weighted EQD2-Comparison**
			SRT		Protons		SRT		Protons		Δ (Protons − SRT)*		Wilcoxon test for paired samples
GTV	D_{mean}	[Gy]	**59.6**	[57.0; 61.3]	**59.0**	[57.6; 59.6]	**109.0**	[101.6; 113.6]	**121.7**	[116.9; 123.7]	**12.9**	[10.9; 14.1]	p = ns
	V_{54Gy}	[%]	**100.0**	[100.0; 100.0]	**99.9**	[98.5; 100.0]	**100.0**	[100.0; 100.0]	**99.9**	[98.5; 100.0]	**−0.1**	[−0.3; 0.0]	***p* < 0.01**
Macula	$D_{2\%}$	[Gy]	**44.1**	[5.7; 62.0]	**42.3**	[0.0; 61.1]	**119.1**	[4.5; 222.9]	**133.2**	[0.0; 263.8]	**−5.5**	[−25.8; 45.3]	***p* = 0.04**
Optic nerve	$D_{2\%}$	[Gy]	**20.6**	[1.3; 56.2]	**0.0**	[0.0; 61.1]	**31.5**	[0.7; 186.1]	**0.0**	[0.0; 264.0]	**−18.0**	[−31.8; −4.6]	***p* < 0.01**
	D_{mean}	[Gy]	**6.4**	[0.5; 21.6]	**0.0**	[0.0; 21.6]	**5.2**	[0.3; 34.2]	**0.0**	[0.0; 40.0]	**−4.6**	[−7.5; −2.7]	***p* < 0.01**
	V_{30Gy}	[%]	**0.0**	[0.0; 34.1]	**0.0**	[0.0; 37.0]	**0.1**	[0.0; 34.1]	**0.0**	[0.0; 37.0]	**0**	[−2.9; 0.0]	***p* < 0.01**
Optic disc	D_{mean}	[Gy]	**20.5**	[1.4; 59.5]	**0.7**	[0.0; 59.6]	**31.3**	[0.8; 206.9]	**0.4**	[0.0; 251.6]	**−21.4**	[−45.7; −12.9]	***p* < 0.01**
Anterior segment	$D_{2\%}$	[Gy]	**17.3**	[5.1; 60.8]	**46.7**	[0.0; 59.7]	**23.6**	[3.9; 215.6]	**157.3**	[0.0; 252.3]	**114.5**	[48.4; 140.6]	***p* < 0.01**
	D_{mean}	[Gy]	**8.1**	[1.3; 41.3]	**14.5**	[0.0; 49.1]	**7.3**	[0.7; 105.7]	**20.4**	[0.0; 175.5]	**9.0**	[−4.8; 43.0]	***p* < 0.01**
Retina	$D_{20\%}$	[Gy]	**43.5**	[17.5; 56.4]	**41.5**	[0.0; 57.6]	**116.3**	[24.1; 187.2]	**125.8**	[0.0; 236.1]	**16.0**	[−27.5; 51.0]	p = ns
	V_{5Gy}	[%]	**87.3**	[55.1; 100.0]	**28.6**	[8.3; 53.6]	**87.3**	[55.1; 100.0]	**28.6**	[8.3; 53.6]	**−53.7**	[−62.5; −46.3]	***p* < 0.01**
	V_{10Gy}	[%]	**60.9**	[34.0; 100.0]	**28.2**	[8.1; 51.6]	**60.9**	[34.0; 100.0]	**28.2**	[8.1; 51.6]	**−32.7**	[−39.1; −26.4]	***p* < 0.01**
	V_{20Gy}	[%]	**39.3**	[17.1; 85.7]	**27.7**	[7.8; 50.3]	**39.3**	[17.1; 85.7]	**27.7**	[7.8; 50.3]	**−13.5**	[−16.7; −9.5]	***p* < 0.01**
	V_{30Gy}	[%]	**30.1**	[11.2; 54.3]	**25.5**	[7.3; 48.6]	**30.1**	[11.2; 54.3]	**25.5**	[7.3; 48.6]	**−4.9**	[−8.0; −1.9]	***p* < 0.01**
Lacrimal gland	$D_{2\%}$	[Gy]	**29.2**	[1.9; 58.1]	**0.0**	[0.0; 61.0]	**51.6**	[1.3; 169.8]	**0.1**	[0.1; 222.6]	**−9.1**	[−32.2; 21.1]	p = ns
	D_{mean}	[Gy]	**16.7**	[0.6; 45.9]	**0.0**	[0.0; 56.6]	**21.2**	[0.4; 111.6]	**0.0**	[0.0; 194.1]	**−15.3**	[−27.7; −4.0]	***p* < 0.01**

* In respect to the organs-at-risk, negative values are favorable to proton therapy.
Abbreviations: SRT = fractionated stereotactic radiotherapy; GTV = gross tumor volume; ns = non-significant; IQR = Interquartile range.

position. A physical wedge and/or combined with the use of a bolus can also reduce dose in specific cases [56,58].

Neovascular glaucoma may lead to enucleation after radiotherapy, generally triggered following local recurrence, tumor necrosis followed by toxic tumor syndrome, and/or painful neovascular glaucoma [37,59,60], all caused by radiation damages to the anterior chamber, but also to the posterior chamber [16,59,61,62]. Overall, RBE-weighted EQD2-median $D_{2\%}$ and D_{mean} values to the anterior segment were always better in SRT. Looking at both segments, protons demonstrated dosimetric advantage in 9/66 patients, with 8 patients having tumors located further than 3-mm from the optic nerve, similar to literature [60]. Both distances to organs-at-risk and dose-volume parameters should be considered for the best treatment option selection regarding the risk of neovascular glaucoma. Additionally, employing multiple beams with protons instead of a single one, as recently suggested [39], might be a promising approach for improved sparing of the anterior region.

For radiation-induced retinopathy (Profile III), our data revealed better retina volume sparing with protons, especially for higher tumor stages (Fig. 3). Retinopathy has high incidence rates after any radiotherapy [22,63], depending on the total dose, fractionation, tumor diameter, and retina dose [40,64–66]. The tumor diameter may be an indirect indicator of the amount of retina surface irradiated. Mercator dose projection maps were used to better understand the geographical location of the dose. The concept is similar to the retinal diagram originally proposed for episcleral brachytherapy where a rasterized polar retina map is displayed along with the isodoses [67] and in conjunction with fundus image it can better identify the retina area at risk of damage [68]. The retinal diagram represents a 2D surface mapping of a sphere, applicable for geometrical model-based ocular treatment. Retina contoured on CT images is, however, irregular. Unfolding an irregularly shaped 3D retina into a 2D surface map is not a trivial task. Mercator maps enable patient-specific evaluation and therefore may be more accurate for dose-toxicity relationship studies for radiation-induced retinopathy than retinal diagrams.

Eye dryness (Profile IV) is mainly due to radiation damage of the lacrimal gland. For protons, due to the sharpness of the penumbrae, reducing the lacrimal gland dose was achievable compared to the SRT doses. It is note-worthy that additional research could enhance lacrimal gland and eyelid dose sparing during proton therapy. For instance, the

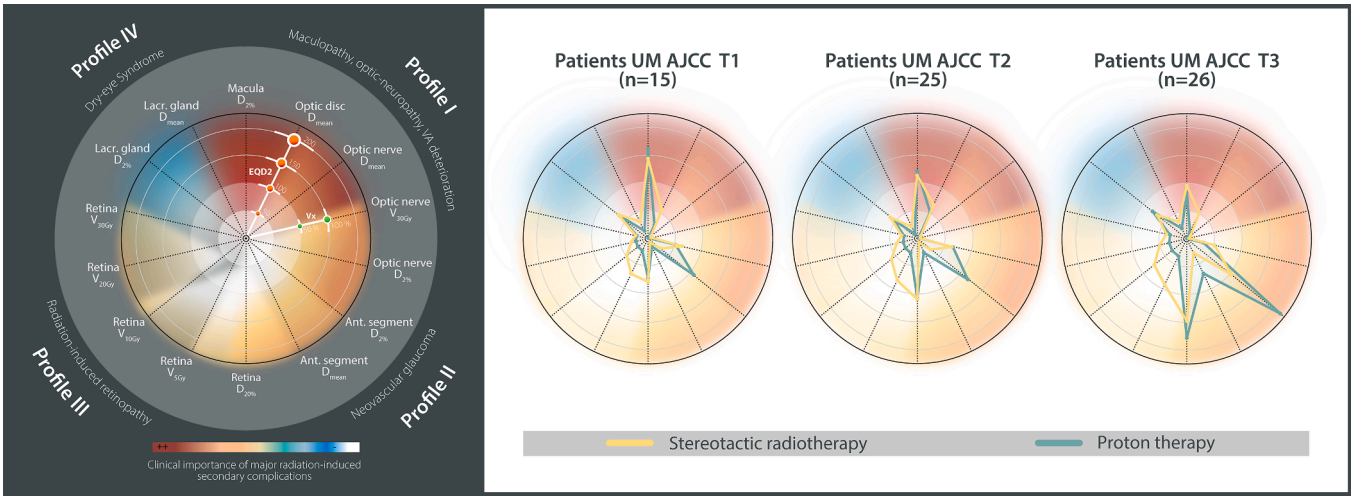

Fig. 3. AJCC-based dosimetric spider maps. Left panel) Graphical representation of dose-volume metrics for every parameter included into each toxicity-specific Profile I to IV. Concentric rings are scaled in RBE-weighted EQD2 dose (in Gy), or percentage of irradiated volume (Vx, %-point). The severity ranking of complications followed institutional multidisciplinary consensus for stereotactic radiotherapy and proton therapy. **Right panels)** Population-averaged spider maps for T1, T2 and T3 uveal melanoma (UM) patients of the cohort. Dose-volume metric values are expressed for a total treatment dose and displayed for fractionated stereotactic radiotherapy plans (in yellow) and proton plans (in green). (For interpretation of the references to colour in this figure legend, the reader is referred to the web version of this article.)

head tilt might be incorporated into the simulation process and be beneficial in some selected cases.

The study has several limitations. Firstly, as UM is a rare disease, a small number of patients was available, limiting generalization of conclusion. Similar comparisons with even smaller number of patients were performed previously by Höcht *et al* [50] (ten patients) and Weber *et al* [49] (one simulated patient). Secondly, the patient selection (single-institute SRT) may introduce bias. Inclusion of other treatment modalities, such as brachytherapy, may alter the conclusions, especially for small tumors where brachytherapy is generally the treatment-of-choice. Thirdly, the selection of constraints was based on literature [16,40–42] due to the lack of solid knowledge on dose-volume effects for ocular radiotherapy. Many established dose-volume tolerance levels included in various guidelines, e.g. QUANTEC [53,69] or RTOG [70–72], cannot be applied for hypo-fractionated regimen. Only one normal tissue complication probability model for choroidal melanoma post-proton therapy exits [42]. Additionally, there are significant uncertainties regarding the α/β-ratios for various ocular structures and their radiation-induced effects. A broad spectrum of α/β-values is reported [73], varying from 2.6 and 12.1 Gy across different UM cell lines, thus potentially leading to significant differences in the prescribed RBE-weighted EQDx doses in current clinical radiotherapy. It is important to further explore tissue response data for hypo-fractionated treatments, specifically UM cell lines, concerning different high-dose fractionation schemes with SRT and proton therapy. The investigation of radiation dose achieving the best treatment outcomes in respect to local tumor control or ocular morbidity was beyond the scope of this study. Lastly, the findings of this research were specifically based on the beam properties of the HollandPTC eyeline [44]. It is important to emphasize that variations in beam quality across eyelines, especially in terms of lateral and distal penumbrae, might impact the conclusions of this research [58,74]. Unlike proton eyelines, the beam properties of CyberKnife systems are consistent across different centers [75].

In conclusion, this study represents the first imaging-based comparison for real-life UM patients between SRT and protons. Looking at the population as a whole, protons offer dosimetric advantages over fractionated stereotactic treatments, however there may be individual patients for whom this is not the case. This research supports the necessity for a plan comparison strategy to address differences in toxicities and help ocular oncology teams decide the appropriate treatment choice together with the patient when both options are available.

Funding statement

This research was co-funded by the research program PROTO-NS4Vision (Grant NWO 14654), which was financed by the Netherlands Organization for Scientific Research (NWO), Technology Foundation STW, the Top consortium for Knowledge & Innovation (TKI-HTSM), and Varian, a Siemens Healthineers Company, Palo Alto, California, USA.

CRediT authorship contribution statement

Emmanuelle Fleury: Conceptualization, Methodology, Formal analysis, Writing – original draft. **Jean-Philippe Pignol:** Methodology, Writing – review & editing, Supervision. **Emine Kiliç:** Conceptualization, Validation, Resources, Visualization. **Maaike Milder:** Conceptualization, Validation, Resources, Visualization. **Caroline van Rij:** Conceptualization, Validation, Resources, Visualization. **Nicole Naus:** Conceptualization, Validation, Resources, Visualization. **Serdar Yavuzyigitoglu:** Conceptualization, Validation, Resources, Visualization. **Wilhelm den Toom:** Conceptualization, Validation, Resources, Visualization. **Andras Zolnay:** Conceptualization, Validation, Resources, Visualization. **Kees Spruijt:** Conceptualization, Validation, Resources, Visualization. **Marco van Vulpen:** Conceptualization, Validation, Resources, Visualization. **Petra Trnková:** Writing – review & editing, Supervision. **Mischa Hoogeman:** Project administration, Funding acquisition, Conceptualization, Methodology, Writing – review & editing, Supervision.

Declaration of Competing Interest

The authors declare the following financial interests/personal relationships which may be considered as potential competing interests: **E. Fleury:** The Department of Radiotherapy (Erasmus Medical Center Cancer Institute, The Netherlands) has research collaborations with Elekta AB, Stockholm, Sweden, Accuray Inc., Sunnyvale, CA, USA, Varian, Palo Alto, CA, USA, RaySearch Laboratories, Stockholm, Sweden, outside the submitted work. **Prof. dr. Pignol:** Prof. dr. Pignol was senior vice president, chief medical and technology officer at Accuray Inc., Sunnyvale, CA, USA until February 2023. **Prof. dr. Hoogeman:**

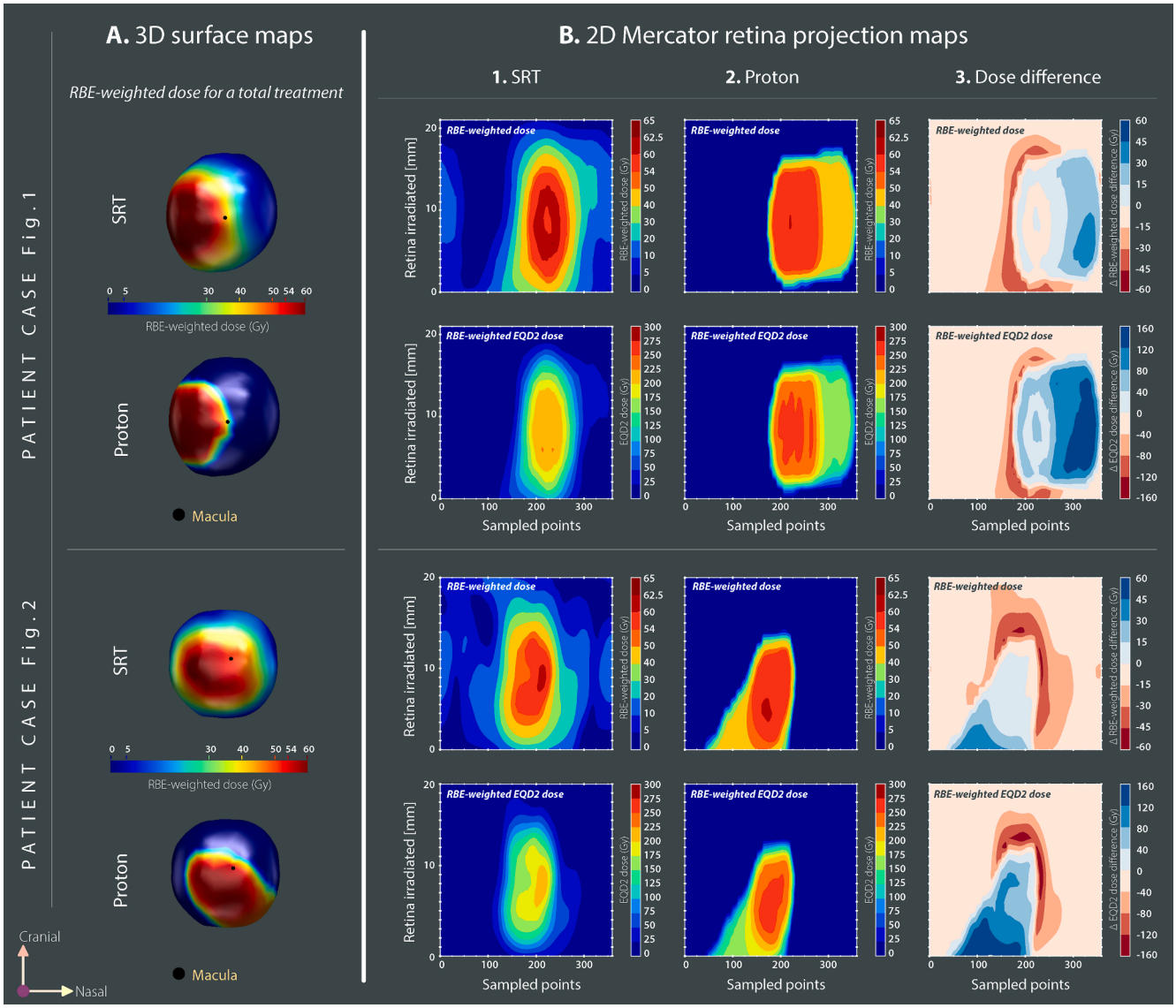

Fig. 4. Retina maps for patients referenced in Fig. 1 and Fig. 2, respectively. **A)** 3D dose surface maps displayed for a total treatment dose for both modalities (RBE-weighted, in Gy). Camera view is located at the back of the eye. **B)** Planar equivalence of the 3D maps. Mercator projection maps are expressed in RBE-weighted dose (upper panels) and when using an equieffective RBE-weighted dose of 2 Gy fractions, EQD2 (lower panels). Y-axis represents the axial slices from caudal to cranial. Numbering of the sampled dose points is performed along the X-axis, a fixed value of 360 equiangular points in each plane of the vitreous body was used. **B.1)** Fractionated stereotactic radiotherapy plan (SRT). **B.2)** Proton plan. **B.3)** Difference between SRT and protons. Negative values (red zones) are in favor of proton therapy. (For interpretation of the references to colour in this figure legend, the reader is referred to the web version of this article.)

Prof. dr. Hoogeman reports grants from Netherlands Organization for Scientific Research, grants from Varian, a Siemens Healthineers Company, Palo Alto, California, USA, during the conduct of the study; being a Member of advisory board Accuray, Sunnyvale, USA; being a participant/presenter at Accuray Thinktank Meeting on Prostate cancer, outside the submitted work; and The Department of Radiotherapy (Erasmus Medical Center Cancer Institute, The Netherlands) has research collaborations with Elekta AB, Stockholm, Sweden, Accuray Inc., Sunnyvale, CA, USA, Varian, Palo Alto, CA, USA, RaySearch Laboratories, Stockholm, Sweden, outside the submitted work.

Acknowledgements

This research was co-funded by the research program PROTON-NS4Vision (Grant NWO 14654), which was financed by the Netherlands Organization for Scientific Research (NWO), Technology Foundation STW, the Top consortium for Knowledge & Innovation (TKI-HTSM), and Varian, a Siemens Healthineers Company, Palo Alto, California, USA.

Appendix A. Supplementary data

Supplementary data to this article can be found online at https://doi.org/10.1016/j.phro.2024.100605.

References

[1] Eibl-Lindner K, Fürweger C, Nentwich M, Foerster P, Wowra B, Schaller U, et al. Robotic radiosurgery for the treatment of medium and large uveal melanoma. Melanoma Res 2016;26:51–7. https://doi.org/10.1097/CMR.0000000000000199.
[2] Akbaba S, Foerster R, Nicolay NH, Arians N, Bostel T, Debus J, et al. Linear accelerator-based stereotactic fractionated photon radiotherapy as an eye-conserving treatment for uveal melanoma. Radiat Oncol 2018;13:140. https://doi.org/10.1186/s13014-018-1088-9.
[3] Zehetmayer M, Kitz K, Menapace R, Ertl A, Heinzl H, Ruhswurm I, et al. Local tumor control and morbidity after one to three fractions of stereotactic external beam irradiation for uveal melanoma. Radiother Oncol 2000;55:135–44. https://doi.org/10.1016/S0167-8140(00)00164-X.

[4] Bellmann C, Fuss M, Holz FG, Debus J, Rohrschneider VHE, et al. Stereotactic radiation therapy for malignant choroidal tumors: Preliminary, short-term results. Ophthalmology 2000;107:358–65. https://doi.org/10.1016/S0161-6420(99)00081-0.

[5] Al-Wassia R, Dal Pra A, Shun K, Shaban A, Corriveau C, Edelstein C, et al. Stereotactic fractionated radiotherapy in the treatment of juxtapapillary choroidal melanoma: the McGill University experience. Int J Radiat Oncol Biol Phys 2011;81:e455–62. https://doi.org/10.1016/J.IJROBP.2011.05.012.

[6] Krema H, Somani S, Sahgal A, Xu W, Heydarian M, Payne D, et al. Stereotactic radiotherapy for treatment of juxtapapillary choroidal melanoma: 3-year follow-up. Br J Ophthalmol 2009;93:1172–6. https://doi.org/10.1136/BJO.2008.153429.

[7] Dunavoelgyi R, Dieckmann K, Gleiss A, Sacu S, Kircher K, Georgopoulos M, et al. Local tumor control, visual acuity, and survival after hypofractionated stereotactic photon radiotherapy of choroidal melanoma in 212 patients treated between 1997 and 2007. Int J Radiat Oncol Biol Phys 2011;81:199–205. https://doi.org/10.1016/j.ijrobp.2010.04.035.

[8] Georg D, Dieckmann K, Bogner J, Zehetmayer M, Pötter R. Impact of a micromultileaf collimator on stereotactic radiotherapy of uveal melanoma. Int J Radiat Oncol Biol Phys 2003;55:881–91. https://doi.org/10.1016/S0360-3016(02)04119-6.

[9] Dieckmann K, Georg D, Bogner J, Zehetmayer M, Petersch B, Chorvat M, et al. Optimizing LINAC-based stereotactic radiotherapy of uveal melanomas: 7 years' clinical experience. Int J Radiat Oncol 2006;66:S47–52. https://doi.org/10.1016/J.IJROBP.2006.01.005.

[10] Eibenberger K, Dunavoelgyi R, Gleiss A, Sedova A, Georg D, Pötter R, et al. Hypofractionated stereotactic photon radiotherapy of choroidal melanoma: 20-year experience. Acta Oncol 2021;60:207–14. https://doi.org/10.1080/0284186X.2020.1820572.

[11] Dunavoelgyi R, Dieckmann K, Gleiss A, Sacu S, Kircher K, Georgopoulos M, et al. Radiogenic side effects after hypofractionated stereotactic photon radiotherapy of choroidal melanoma in 212 patients treated between 1997 and 2007. Int J Radiat Oncol Biol Phys 2012;83:121–8. https://doi.org/10.1016/J.IJROBP.2011.06.1957.

[12] Health Council of the Netherlands. Proton radiotherapy. Horizon scanning report. The Hague: Health Council of the Netherlands 2009, publication no. 2009/17E.

[13] Dendale R, Lumbroso-Le Rouic L, Noel G, Feuvret L, Levy C, Delacroix S, et al. Proton beam radiotherapy for uveal melanoma: Results of Curie Institut-Orsay Proton Therapy Center (ICPO). Int J Radiat Oncol Biol Phys 2006;65:780–7. https://doi.org/10.1016/j.ijrobp.2006.01.020.

[14] Damato B, Kacperek A, Chopra M, Campbell IR, Errington RD. Proton beam radiotherapy of choroidal melanoma: The Liverpool-Clatterbridge experience. Int J Radiat Oncol Biol Phys 2005;62:1405–11. https://doi.org/10.1016/j.ijrobp.2005.01.016.

[15] Gragoudas E, Li W, Goitein M, Lane AM, Munzenrider JE, Egan KM. Evidence-Based Estimates of Outcome in Patients Irradiated for Intraocular Melanoma. Arch Ophthalmol 2002;120:1665–71. https://doi.org/10.1001/ARCHOPHT.120.12.1665.

[16] Mishra KK, Daftari IK, Weinberg V, Cole T, Quivey JM, Castro JR, et al. Risk factors for neovascular glaucoma after proton beam therapy of uveal melanoma: A detailed analysis of tumor and dose-volume parameters. Int J Radiat Oncol Biol Phys 2013;87:330–6. https://doi.org/10.1016/j.ijrobp.2013.05.051.

[17] Bensoussan TJ, Maschi C, Dalas J, Dan Schouver E, et al. Outcomes after Proton Beam Therapy for Large Choroidal Melanomas in 492 Patients. Am J Ophthalmol 2016;165:78–87. https://doi.org/10.1016/j.ajo.2016.02.027.

[18] Karimi S, Arabi A, Siavashpour Z, Shahraki T, Ansari I. Efficacy and complications of ruthenium-106 brachytherapy for uveal melanoma: a systematic review and meta-analysis. J Contemp Brachytherapy 2021;13:358–64. https://doi.org/10.5114/jcb.2021.106191.

[19] Sagoo MS, Shields CL, Emrich J, Mashayekhi A, Komarnicky L, Shields JA. Plaque radiotherapy for juxtapapillary choroidal melanoma: Treatment complications and visual outcomes in 650 consecutive cases. JAMA Ophthalmol 2014;132:697–702. https://doi.org/10.1001/jamaophthalmol.2014.111.

[20] Marinkovic M, Horeweg N, Fiocco M, Peters FP, Sommers LW, Laman MS, et al. Ruthenium-106 brachytherapy for choroidal melanoma without transpupillary thermotherapy: Similar efficacy with improved visual outcome. Eur J Cancer 2016;68:106–13. https://doi.org/10.1016/j.ejca.2016.09.009.

[21] Marinkovic M, Horeweg N, Laman MS, Bleeker JC, Ketelaars M, Peters FP, et al. Ruthenium-106 brachytherapy for iris and iridociliary melanomas. Br J Ophthalmol 2018;102:1154–9. https://doi.org/10.1136/bjophthalmol-2017-310688.

[22] Liegl R, Schmelter V, Fuerweger C, Ehret F, Priglinger S, Muacevic A, et al. Robotic CyberKnife Radiosurgery for the Treatment of Choroidal and Ciliary Body Melanoma. Am J Ophthalmol 2023;250:177–85. https://doi.org/10.1016/J.AJO.2022.12.021.

[23] Muller K, Naus N, Nowak PJ, Schmitz PI, de Pan C, van Santen CA, et al. Fractionated stereotactic radiotherapy for uveal melanoma, late clinical results. Radiother Oncol 2012;102:219–24. https://doi.org/10.1016/j.radonc.2011.06.038.

[24] Messineo D, Barile G, Morrone S, La Torre G, Turchetti P, Accetta L, et al. Meta-analysis on the utility of radiotherapy for the treatment of Ocular Melanoma. Clin Ter 2020;171:e94–6. https://doi.org/10.7417/CT.2020.2195.

[25] Kosydar S, Robertson JC, Woodfin M, Mayr NA, Sahgal A, Timmerman RD et al. Systematic Review and Meta-Analysis on the Use of Photon-based Stereotactic Radiosurgery Versus Fractionated Stereotactic Radiotherapy for the Treatment of Uveal Melanoma. Am J Clin Oncol; 44:32–42. doi: 10.1097/COC.0000000000000775.

[26] Zemba M, Dumitrescu OM, Gheorghe AG, Radu M, Ionescu MA, Vatafu A, et al. Ocular Complications of Radiotherapy in Uveal Melanoma. Cancers 2023;15:333. https://doi.org/10.3390/cancers15020333.

[27] Thariat J, Martel A, Matet A, Loria O, Kodjikian L, Nguyen AM, et al. Non-Cancer Effects following Ionizing Irradiation Involving the Eye and Orbit. Cancers 2022;14:1194. https://doi.org/10.3390/CANCERS14051194.

[28] Goitein M, Miller T. Planning proton therapy of the eye. Med Phys 1983;10:275–83. https://doi.org/10.1118/1.595258.

[29] Kivelä T, Simpson R, Grossniklaus H. Uveal melanoma. In: AJCC Cancer Staging Manual. 8th ed.,. Springer; 2016. p. 805–17.

[30] Wilke L, Andratschke N, Blanck O, Brunner TB, Combs SE, Grosu AL, et al. ICRU report 91 on prescribing, recording, and reporting of stereotactic treatments with small photon beams. Strahlenther Onkol 2019;195:193–8. https://doi.org/10.1007/s00066-018-1416-x.

[31] Muller K, Nowak PJCM, Luyten GPM, Marijnissen JP, De Pan C, Levendag P. A modified relocatable stereotactic frame for irradiation of eye melanoma: Design and evaluation of treatment accuracy. Int J Radiat Oncol Biol Phys 2004;58:284–91. https://doi.org/10.1016/j.ijrobp.2003.08.029.

[32] ICRU Report 78: Prescribing, Recording, and Reporting Proton-Beam Therapy. Int Comm Radiat Units Mea 2007.

[33] Kacperek A. Protontherapy of eye tumours in the UK: A review of treatment at Clatterbridge. Appl Radiat Isot 2008;67:378–86. https://doi.org/10.1016/J.APRADISO.2008.06.012.

[34] Mishra KK, Daftari IK. Proton therapy for the management of uveal melanoma and other ocular tumors. Chinese Clin Oncol 2016;5:50. https://doi.org/10.21037/cco.2016.07.06.

[35] Egger E, Zografos L, Schalenbourg A, Beati D, Böhringer T, Chamot L, et al. Eye retention after proton beam radiotherapy for uveal melanoma. Int J Radiat Oncol Biol Phys 2003;55:867–80. https://doi.org/10.1016/S0360-3016(02)04200-1.

[36] Sas-Korczynska B, Markiewicz A, Romanowska-Dixon B, Pluta E. Preliminary results of proton radiotherapy for choroidal melanoma - The Kraków experience. Wspolczesna Onkol 2014;18:359–66. https://doi.org/10.5114/wo.2014.42233.

[37] Seibel I, Cordini D, Rehak M, Hager A, Riechardt AI, Böker A. Local Recurrence after Primary Proton Beam Therapy in Uveal Melanoma: Risk Factors, Retreatment Approaches, and Outcome. Am J Ophthalmol 2015;160:628–36. https://doi.org/10.1016/j.ajo.2015.06.017.

[38] Fleury E, Trnková P, Erdal E, Hassan M, Stoel B, Jaarma-Coes M, et al. Three-dimensional MRI-based treatment planning approach for non-invasive ocular proton therapy. Med Phys 2020;48:1315–26. https://doi.org/10.1002/mp.14665.

[39] Fleury E, Trnková P, van Rij C, Rodrigues M, Klaver Y, Spruijt K, et al. Improving organs-at-risk sparing for choroidal melanoma patients: A CT-based two-beam strategy in ocular proton therapy with a dedicated eyeline. Radiother Oncol 2022;171:173–81. https://doi.org/10.1016/j.radonc.2022.04.021.

[40] Riechardt AI, Stroux A, Seibel I, Heufelder J, Zeitz O, Böhmer D, et al. Side effects of proton beam therapy of choroidal melanoma in dependence of the dose to the optic disc and the irradiated length of the optic nerve. Graefes Arch Clin Exp Ophthalmol 2020;258:2523–33. https://doi.org/10.1007/s00417-020-04780-y.

[41] Daftari IK, Char DH, Verhey LJ, Castro JR, Petti PL, Meecham WJ, et al. Anterior segment sparing to reduce charged particle radiotherapy complications in uveal melanoma. Int J Radiat Oncol Biol Phys 1997;1997(39):997–1010. https://doi.org/10.1016/S0360-3016(97)00557-9.

[42] Espensen CA, Kiilgaard JF, Appelt AL, Fog LS, Herault J, Maschi C, et al. Dose-Response and Normal Tissue Complication Probabilities after Proton Therapy for Choroidal Melanoma. Ophthalmology 2021;128:152–61. https://doi.org/10.1016/j.ophtha.2020.06.030.

[43] Slopsema RL, Mamalui M, Zhao T, Yeung D, Malyapa R, Li Z. Dosimetric properties of a proton beamline dedicated to the treatment of ocular disease. Med Phys 2013;41:011707. https://doi.org/10.1118/1.4842455.

[44] Fleury E, Trnková P, Spruijt K, Herault J, Lebbink F, Heufelder J, et al. Characterization of the HollandPTC proton therapy beamline dedicated to uveal melanoma treatment and an interinstitutional comparison. Med Phys 2021;48:4506–22. https://doi.org/10.1002/mp.15024.

[45] Kacperek A. Ocular Proton Therapy Centers. In: Linz U, editor. Ion Beam Therapy. Springer; 2012. p. 149–77. https://doi.org/10.1007/978-3-642-21414-1_10.

[46] Joiner M, Der Van KA. Basic Clinical Radiobiology, Fifth Edit. Taylor & Francis Group: CRC Press; 2018.

[47] Hansen CR, Crijns W, Hussein M, Rossi L, Gallego P, Verbakel W, et al. Radiotherapy Treatment plannINg study Guidelines (RATING): A framework for setting up and reporting on scientific treatment planning studies. Radiother Oncol 2020;153:67–78. https://doi.org/10.1016/j.radonc.2020.09.033.

[48] Hoogeman MS, Van Herk M, De Bois J, Muller-Timmermans P, Koper PCM, Lebesque JV. Quantification of local rectal wall displacements by virtual rectum unfolding. Radiother Oncol 2004;70:21–30. https://doi.org/10.1016/J.RADONC.2003.11.015.

[49] Weber DC, Bogner J, Verwey J, Georg D, Dieckmann K, Escudé L, et al. Proton beam radiotherapy versus fractionated stereotactic radiotherapy for uveal melanomas: A comparative study. Int J Radiat Oncol Biol Phys 2005;63:373–84. https://doi.org/10.1016/j.ijrobp.2005.01.057.

[50] Höcht S, Stark R, Seiler F, Heufelder J, Bechrakis NE, Cordini D, et al. Proton or stereotactic photon irradiation for posterior uveal melanoma? A planning intercomparison. Strahlenther Onkol 2005;181:783–8. https://doi.org/10.1007/s00066-005-1395-6.

[51] Varian Medical Systems, "Planning Reference Guide for Eclipse Ocular Proton Planning Eclipse Ocular Proton Planning," no. September, 2007.

[52] Hussain RN, Chiu A, Pittam B, Taktak A, Damato BE, Kacperek A, et al. Proton beam radiotherapy for choroidal and ciliary body melanoma in the UK-national

audit of referral patterns of 1084 cases. Eye 2023;37:1033–6. https://doi.org/10.1038/s41433-022-02178-0.
[53] Mayo C, Martel MK, Marks LB, Flickinger J, Nam J, Kirkpatrick J. Radiation Dose-Volume Effects of Optic Nerves and Chiasm. Int J Radiat Oncol Biol Phys 2009;76:28–35. https://doi.org/10.1016/j.ijrobp.2009.07.1753.
[54] Toutée A, Angi M, Dureau S, Lévy-Gabriel C, Lumbroso-Le Rouic L, Dendale R, et al. Long-term visual outcomes for small uveal melanoma staged T1 treated by proton beam radiotherapy. Cancers 2019;11:1047. https://doi.org/10.3390/cancers11081047.
[55] Sikuade MJ, Salvi S, Rundle PA, Errington DG, Kacperek A, Rennie IG. Outcomes of treatment with stereotactic radiosurgery or proton beam therapy for choroidal melanoma. Eye 2015;29:1194–8. https://doi.org/10.1038/eye.2015.109.
[56] Thariat J, Grange JD, Mosci C, Rosier L, Maschi C, Lanza F, et al. Visual Outcomes of Parapapillary Uveal Melanomas Following Proton Beam Therapy. Int J Radiat Oncol Biol Phys 2016;95:328–35. https://doi.org/10.1016/j.ijrobp.2015.12.011.
[57] Dunavoelgyi R, Georg D, Zehetmayer M, Schmidt-Erfurth U, Pötter R, Dörr W, et al. Dose-response of critical structures in the posterior eye segment to hypofractioned stereotactic photon radiotherapy of choroidal melanoma. Radiother Oncol 2013;108:348–53. https://doi.org/10.1016/j.radonc.2013.08.018.
[58] Wulff J, Koska B, Janson M, Bäumer C, Denker A, Geismar D, et al. Technical note: Impact of beam properties for uveal melanoma proton therapy—An in silico planning study. Med Phys 2022;49:3481–8. https://doi.org/10.1002/mp.15573.
[59] Conway RM, Poothullil AM, Daftari IK, Weinberg V, Chung JE, O'Brien JM. Estimates of Ocular and Visual Retention Following Treatment of Extra-Large Uveal Melanomas by Proton Beam Radiotherapy. Arch Ophthalmol 2006;124:838–43. https://doi.org/10.1001/ARCHOPHT.124.6.838.
[60] van Beek JGM, Ramdas WD, Angi M, van Rij CM, Naus NC, Kacperek A, et al. Local tumour control and radiation side effects for fractionated stereotactic photon beam radiotherapy compared to proton beam radiotherapy in uveal melanoma. Radiother Oncol 2021;157:219–24. https://doi.org/10.1016/j.radonc.2021.01.030.
[61] Riechardt AI, Pilger D, Cordini D, Seibel I, Gundlach E, Hager A, et al. Neovascular glaucoma after proton beam therapy of choroidal melanoma: incidence and risk factors. Graefes Arch Clin Exp Ophthalmol 2017;255:2263–9. https://doi.org/10.1007/s00417-017-3737-3.
[62] Fernandes BF, Weisbrod D, Yücel YH, Follwell M, Krema H, Heydarian M, et al. Neovascular glaucoma after stereotactic radiotherapy for juxtapapillary choroidal melanoma: Histopathologic and dosimetric findings. Int J Radiat Oncol Biol Phys 2011;80:377–84. https://doi.org/10.1016/j.ijrobp.2010.04.073.
[63] Yazici G, Kiratli H, Ozyigit G, Sari SY, Cengiz M, Tarlan B, et al. Stereotactic Radiosurgery and Fractionated Stereotactic Radiation Therapy for the Treatment of Uveal Melanoma. Int J Radiat Oncol Biol Phys 2017;98:152–8. https://doi.org/10.1016/j.ijrobp.2017.02.017.
[64] Seibel I, Cordini D, Hager A, Tillner J, Riechardt AI, Heufelder J, et al. Predictive risk factors for radiation retinopathy and optic neuropathy after proton beam therapy for uveal melanoma. Graefes Arch Clin Exp Ophthalmol 2016;254:1787–92. https://doi.org/10.1007/s00417-016-3429-4.
[65] Monroe AT, Bhandare N, Morris CG, Mendenhall WM. Preventing radiation retinopathy with hyperfractionation. Int J Radiat Oncol Biol Phys 2005;61:856–64. https://doi.org/10.1016/j.ijrobp.2004.07.664.
[66] Heilemann G, Fetty L, Blaickner M, Nesvacil N, Zehetmayer M, Georg D, et al. Retina dose as a predictor for visual acuity loss in (106)Ru eye plaque brachytherapy of uveal melanomas. Radiother Oncol 2018;127:379–84. https://doi.org/10.1016/j.radonc.2017.11.010.
[67] Astrahan MA. The retina dose-area histogram: A metric for quantitatively comparing rival eye plaque treatment options. J Contemp Brachytherapy 2013;5:23–32. https://doi.org/10.5114/jcb.2013.34450.
[68] Daftari IK, Mishra KK, O'Brien JM, Tsai T, Park SS, Sheen M, et al. Fundus image fusion in EYEPLAN software: An evaluation of a novel technique for ocular melanoma radiation treatment planning. Med Phys 2010;37:5199–207. https://doi.org/10.1118/1.3488891.
[69] Bentzen SM, Constine LS, Deasy JO, Eisbruch A, Jackson A, Marks LB, et al. Quantitative Analyses of Normal Tissue Effects in the Clinic (QUANTEC): An Introduction to the Scientific Issues. Int J Radiat Oncol Biol Phys 2010;76:3–9. https://doi.org/10.1016/j.ijrobp.2009.09.040.
[70] Noël G, Le Fèvre C, Antoni D. Delineation of organs at risk. Cancer/Radiotherapie 2022;26:76–91. https://doi.org/10.1016/j.canrad.2021.08.001.
[71] Marchand V, Dendale R. Dose de tolérance à l'irradiation des tissus sains: l'œil. Cancer/Radiotherapie 2010;14:277–83. https://doi.org/10.1016/j.canrad.2010.03.008.
[72] Scoccianti S, Detti B, Gadda D, Greto D, Furfaro I, Meacci F, et al. Organs at risk in the brain and their dose-constraints in adults and in children: A radiation oncologist's guide for delineation in everyday practice. Radiother Oncol 2015;114:230–8. https://doi.org/10.1016/j.radonc.2015.01.016.
[73] Calipel A, Lux AL, Guérin S, Lefaix JL, Laurent C, Bernaudin M, et al. Differential radiosensitivity of uveal melanoma cell lines after X-rays or carbon ions radiation. Inves Ophthalmol Vis Sci 2015;56:3085–94. https://doi.org/10.1167/iovs.14-15930.
[74] Gerard A, Peyrichon ML, Vidal M, Barnel C, Sauerwein W, Carnicer A, et al. Ocular proton therapy, pencil beam scanning high energy proton therapy or stereotactic radiotherapy for uveal melanoma; an in silico study. Cancer Radiother 2022;26:1027–33. https://doi.org/10.1016/j.canrad.2022.03.003.
[75] Sharma SC, Ott JT, Williams JB, Dickow D. Commissioning and acceptance testing of a CyberKnife linear accelerator. J Appl Clin Med Phys 2007;8:119–25. https://doi.org/10.1120/jacmp.v8i3.2473.